Influence of Hydrogen Incorporation on the Structure and Stoichiometry of Chemically Vapor Deposited Silica Films

F. Ojeda, I. Montero, F. Abel,† and J. M. Albella*

Departamento de Física e Ingeniería de Superficies, Instituto de Ciencia de Materiales de Madrid, CSIC, Cantoblanco, 28049 Madrid, Spain

Received February 1, 2001. Revised Manuscript Received May 7, 2001

Hydrogen incorporation into SiO_2 films grown by low-pressure chemical vapor deposition (CVD) from SiH_4/O_2 mixtures is investigated by means of infrared spectroscopy (IRS), nuclear magnetic resonance (NMR), elastic recoil detection analysis (ERDA), X-ray photoemission spectroscopy (XPS), and nuclear reaction analysis (NRA). We find that hydrogen atoms are preferentially bonded to O atoms, forming bulk SiOH groups, either isolated or clustered, and H_2O groups, with a minor incorporation of SiH groups, as well as geminal and surface isolated SiOH groups. The proportion of clustered SiOH groups decreases upon increasing the deposition temperature, which has been attributed to the faster dehydroxylation reactions and higher surface mobility of the hydrogenated species involved in the film growth. Using a novel method based on the combination of NRA and ERDA, we verify quantitatively that the predominance of O−H over Si−H bonding implies a slight overstoichiometric character (O/Si atomic ratio > 2) that is accentuated with increasing OH concentration.

Introduction

Hydrogen incorporation into SiO_2 films grown by chemical vapor deposition (CVD) techniques is the main impediment to obtain as-deposited films with structural characteristics close to those obtained by the thermal oxidation of silicon at high temperatures.[1] Nonbridging SiOH and SiH groups break the network continuity and thus are generally associated with the presence of porous structures in the oxide matrix.[2−5] Parasitic capacitance, low breakdown field, and high dielectrical permittivity are frequent nondesirable characteristics in hydrogenated oxides.[6,7] Hydrogen incorporation results also in low refractive indexes for SiO_2-based optical coatings, increased diffuse reflection, and important losses in optical fiber transmissions.[2,4,8−10] In addition, SiO_2-based ceramic membranes for hot gas separation in industrial processes under aggressive conditions, such as those imposed by coal gasification cycles, are required to be thermally and chemically stable.[11,12] Obviously, the requirements for all these applications are compromised by the incorporation of SiOH and SiH groups into the oxide matrix.[2,13]

Despite these disadvantages, hydrogen incorporation into SiO_2 can be exploited to prepare porous nanostructured materials with interesting applications in the domain of gas and liquid separation[14] as well as in the manufacture of ultra-large-scale integrated solid-state devices.[15] Moreover, SiOH surface groups, which provide silica surface with a high reactivity, are important active sites during the growth of silica[16−18] and play a key role in many applications in the field of analytical chemistry, catalysis, and biochemistry.[19] For all these reasons, a fundamental understanding of the mechanisms determining the location of hydrogen in the oxide matrix and its final concentration is needed.

Silicon oxide films are frequently obtained by chemical vapor deposition (CVD) from the SiH_4/O_2 reaction, since this technique provides high-quality oxides and the capability for achieving reasonable deposition rates at relatively low temperatures (typically between 300 and 450 °C).[20] At present, there is little question that the ultimate reason for the low-temperature character

* To whom correspondence should be addressed. Phone: 34 91 3349080. Fax: 34 91 3720623. E-mail: albella@icmm.csic.es.

† Groupe de Physique des Solides, Universités Paris 7 et Paris 6, Unité associée au CNRS UMR 7588, 2 Place Jussieu, 75251 Paris Cedex 05, France.

(1) Makabe, M.; Hirose, K.; Ishikawa, H.; Ono, H.; Ishitani, A.; Mizuki, J. *Beam-Solid Interactions for Materials Synthesis and Characterization, Mater. Res. Soc. Symp. Proc.* **1995**, *354*, 455.

(2) Pliskin, W. A.; Lehman, H. S. J. *Electrochem. Soc* **1965**, *112*, 1013.

(3) Lange, P.; Shnakenerg, U.; Ullerich, S.; Schliwinski, H.-J. *J. Appl. Phys.* **1990**, *68*, 3532.

(4) Najmi, O.; Montero, I.; Galán, L.; Perrière, J.; Albella, J. M. *Appl. Surf. Sci.* **1993**, *70/71*, 217.

(5) Montero, I.; Galán, L.; Najmi, O.; Albella, J. M. *Phys. Rev. B* **1994**, *50*, 4881.

(6) Liehr, M.; Cohen, S. A. *Appl. Phys. Lett.* **1992**, *60*, 198.

(7) Han, S. M.; Aydil, E. S. *Thin Solid Films* **1996**, *290−291*, 427.

(8) Goullet, A.; Charles, C.; García, P.; Turban, G. *J. Appl. Phys.* **1993**, *74*, 6876.

(9) Griscom, D. L. *MRS Bull.* 1987, June 16/August 15, 20.

(10) Ferendeci, A. M. *Physical Foundations of Solid State and Electron Devices*; McGraw-Hill: New York, 1991.

(11) Alvin, M. A.; Lippert, T. E.; Lane J. E. *Ceram. Bull.* **1991**, *70*, 1491.

(12) Egan, B. Z.; Fain, D. E.; Roettger, G. E.; White D. E. *J. Eng. Gas Turb. Power* **1992**, *114*, 367.

(13) Huffman, M.; Navrotsky, A.; Pintchovski, F. S. *J. Electrochem. Soc.* **1986**, *133*, 164.

(14) Lange, R. S. A.; Kekkink, J. H. A.; Keizer, K.; Burggraaf, A. J. *Key Eng. Mater.* **1991**, *61−62*, 77.

(15) Jin, C.; Luttmer, J. D.; Smith, D. M.; Ramos, T. A. *MRS Bull.* **1997**, *22*(10), 39.

(16) Iler, R. K. *The Chemistry of Silica;* Wiley: New York, 1979.

(17) Hair, M. L.; Hertl, W. *J. Phys. Chem.* **1969**, *73*, 4269.

(18) Hobza, P.; Sauer, J.; Morgeneyer, C.; Hurych, J.; Zahradnik, R. *J. Phys. Chem.* **1981**, *85*, 4061.

(19) Van Der Voort, P.; Vansant, E. F. *J. Liq. Chrom., Relat. Technol.* **1996**, *19*, 2723.

10.1021/cm011040k CCC: $20.00
Published on Web 09/20/2001

of silane oxidation is the formation, through homogeneous branching-chain reactions, of highly reactive species such as SiH_3, H, O, OH, and HO_2 radicals.[21−24] Parallel to the production of these radicals, precursor species with the general formula SiO_mH_n are also formed in the gas phase.[6,23,24] To date, the identity of the SiO_mH_n species and the chemical mechanisms through which they are formed have not been clarified. What it is known is that a certain amount of these hydrogenated species are trapped by the growing oxide film without being completely dehydrogenated, leading to nonnegligible concentrations of SiOH, SiH, and H_2O groups in the films.[3,6,24−27]

The main goal of this work is to study the incorporation of hydrogenated species formed during the SiH_4/O_2 reaction into the resulting film. Chemical bonding of hydrogen and its concentration in the oxide film have been studied by different structural and analytical techniques. As will be shown by this work, the small departures from the stoichiometric composition (SiO_2) to which silica films are subjected are mostly determined by the type of hydrogen bonding in the oxide matrix. Unfortunately, most analytical techniques are unable to give precise measurements of the oxide stoichiometry, due to the small deviations induced by hydrogen in the oxide composition and to different experimental limitations inherent to them (e.g., surface sensibility and alterations of sample composition and structure). For this reason, one of the most important challenges of this work is to obtain a reliable estimation of the oxide stoichiometry. For this purpose, we have employed a novel method based on the combination of nuclear reaction analysis with conventional elastic recoil detection analysis. The main advantage of this method over others commonly used in SiO_2 characterization lies in the possibility of determining the whole bulk oxide composition (O/Si and H/Si atomic ratios) from consecutive measurements taken in the same vacuum chamber and from the same zone of each sample, which minimizes significant experimental errors related to sample degradation and lateral inhomogeneities.

Experimental Section

Hydrogenated silicon oxide (SiO_xH_y) thin films were chemically vapor deposited on monocrystalline (100) oriented silicon wafers (Virginia Semiconductors) polished on both faces. The deposition system was a low-pressure hot-wall horizontal CVD reactor.[24] This reactor was fabricated from a quartz tube with an inner diameter of 6.1 cm and a total length of 100 cm. The length of the heating zone, which is centered in a 30 cm long cylindrical furnace, is 10 cm. A horizontal graphite plate was used as substrate-holder. The flow of the reactants, SiH_4 (diluted at 2% in N_2, 99.999% purity) and O_2 (99.9992% purity), was adjusted by means of mass flow controllers. Low-pressure conditions were achieved by means of a vacuum system that consists of a rotary pump boosted by a Roots pump. The base pressure was 5×10^{-4} Torr. The process pressure was measured by a capacitative gauge and controlled by means of an electronically driven butterfly valve. SiO_xH_y films were also deposited on (100) oriented GaAs wafers and Ta plates using a low-pressure cold-wall CVD reactor described elsewhere.[28] Both GaAs wafers and Ta plates were used instead of silicon in the Si(d,p) NRA measurements described below in order to avoid the substrate contribution. The deposition rate was estimated from thickness measurements obtained by means of a profilometer (Dektak 3030). In all deposition experiments, the thickness of the films, which ranged from 0.1 up to 57 μm, increased linearly with deposition time. As-deposited films were characterized ex situ by different analytical techniques.

IRS (infrared spectroscopy) was employed to study the chemical bonding in the films. IR-transmittance (T) spectra were recorded using a double-beam dispersive spectrophotometer (Hitachi 270−50) in normal incidence mode within the 4000−250 cm^{-1} range. To perform quantitative analysis, these spectra were converted into absorbance (A) spectra through the relation $A = -\log(T)$.

High-resolution solid-state ^{29}Si cross-polarization magic angle spinning nuclear magnetic resonance (CP/MAS NMR) of powdered SiO_xH_y samples were recorded at 79.49 MHz, by spinning the samples at the magic angle (54°7′) in a Bruker MSL-400 spectrometer equipped with a Fourier transform unit. The spinning frequency was 4000 cps. SiO_xH_y films of about 150 mg were deposited on monocrystalline NaCl substrates, further recovered by ultrasound-enhanced dilution of NaCl in H_2O (5 min long), blown with dry N_2, and, finally, carefully packed in ZrO_2 rotors. No change was detected in the IR spectra of these films after the dilution/drying process, which could respond to their extremely low surface area (<0.03 m^2/g) and water diffusivity at room temperature (<10^{-12} cm^2/s).[29] For the same reasons, the effect of this process on the NMR measurements can be considered negligible. The standard CP/MAS pulse sequence was applied with a 6.5 μs ^1H − 90° pulse width, 3 ms contact pulses, and 5 s repetition times, being the spectral width 10^5 Hz. Chemical shifts are given with respect to the TMS signal. Accumulations amounted to 5000 free induction decays (FID).

XPS (X-ray photoelectron spectroscopy) analysis was performed with a VGS ESCALAB 210 instrument using nonmonochromatic Mg Kα X-radiation ($h\nu$ = 1253.6 eV). XPS allows us to identify elements and chemical states present in the outermost ∼5 nm at the surface of the samples. The average near-surface composition, O/Si atomic ratio, has been calculated using the XPS peak intensities and the corresponding XPS sensitivity factors of the Si 2p and O 1s core levels.[30] Intensities were determined from the integrated areas under the fitted peaks. A mixed Gaussian−Lorentzian peak shape was used. Since XPS intensities are proportional to element concentration (number of atoms per analyzed volume) and intensity ratios were used for the quantitative analysis, the results refer to atomic ratios, i.e., the number of atoms of a chemical species divided by the total number of atoms in the analyzed volume. The pressure in the UHV analytical chamber was ∼10^{-10} Torr. The analyzer was operated in the constant-pass energy mode, being 20 eV for the core level spectra. The resolution of the electron-energy analyzer was ∼0.5 eV. Previous to the XPS measurements, the sample surface was cleaned with 2 kV Ar^+ ion bombardment using a differentially pumped ion gun and 5×10^{-7} Torr in the analyzer chamber. This cleaning process, designed to minimize the surface damage, was maintained until the C 1s signal, due to the surface pollution on the sample, was completely eliminated from the

(20) Jensen, K. F.; Kern, W. *Thin Film Processes II*; Vossen, J. L., Kern, W., Eds.; Academic Press: Boston, 1991.
(21) Vasilyeva, L. L.; Drozdov, V. N.; Repinsky, S. M.; Svitashev, K. K. *Thin Solid Films* **1978**, *55*, 221.
(22) van de Weijer, P.; Zwerver, B. H. *Chem. Phys. Lett.* **1989**, *163*, 48.
(23) Takahashi, T.; Hagiwara, K.; Egashira, Y.; Komiyama, H. *J. Electrochem. Soc* **1996**, *143*, 1355.
(24) Ojeda, F.; Castro-García, A.; Gómez-Aleixandre, C.; Albella, J. M. *J. Mater. Res.* **1998**, *13*, 2308.
(25) Taft, E. A. *J. Electrochem. Soc.* **1979**, *126*, 1728.
(26) Nishino, S.; Honda, H.; Matsunami, H. *Jpn. J. Appl. Phys.* **1986**, *25*, L87-L89.
(27) Katz, A.; Feingold, A.; Chakrabarti, U. K.; Pearton, S. *J. Appl. Phys. Lett.* **1991**, *59*, 2552.
(28) Ojeda, F.; Albella, J. M., *Electrochemical Society Proceedings, Fundamental Gas-Phase and Surface Chemistry of Vapor-Phase Materials Synthesis*, **1999**, *98−23*, 233.
(29) Doremus, R. H. *J. Mater. Res.* **1995**, *10*, 2379.
(30) *XPS sensitivity factors Data Sheet supplied by Leybold-Heraeus with a LH 10 ESCA spectrometer*, 1985, corrected for transmission function of VGS ESCALAB instrument.

XPS spectra. In this way we ensure that the XPS measurements are not affected by the sample exposure to the ambient pollution, including water, after the deposition process.

ERDA (elastic recoil detection analysis) was performed in the 2.5 MeV Van de Graaf accelerator at the Groupe de Physique des Solides.[31,32] A monochromatic ^{4}He beam with energies ranging from 1.9 up to 2.2 MeV was used in the usual ERDA geometry (75° tilt of the samples). A 10 μm Mylar absorber was placed in front of the Si surface barrier detector, located at $\theta_{lab} = 30°$, to stop the forward scattered ^{4}He particles. Energy and composition calibrations were performed by means of totally hydrogenated, $(C_8H_8)_n$, and deuterated, $(C_8D_8)_n$, polystyrene thin film references prepared by spin-coating. These references targets are stable enough under our experimental conditions to be used as standard targets for hydrogen quantitative analysis.[33] The H content of these samples was determined via their carbon content using the procedure described in ref 34. The stability of the SiO_2 samples was checked by means of a multichannel analyzer. The results presented in this work correspond exclusively to samples showing hydrogen losses lower than 5%.

NRA (nuclear reaction analysis) was carried out in the same ion beam facilities used for the ERDA experiments. Oxygen content was determined by the $^{16}O(d,p_1)^{17}O$ nuclear reaction. The energy of the deuterium beam was set at 857 keV and the detection angle θ_{lab} at 150°. Below this energy the reaction cross section shows a 50 keV wide plateau, which provides measurements with a precision better than 4% without any correction for oxygen contents less than 7×10^{18} cm^{-2} (equivalent to 1.6 μm of 2.2 g/cm^3 dense SiO_2). A Ta_2O_5 thin film grown by anodic oxidation of tantalum was used as reference target. The silicon content of the films deposited on the GaAs and Ta substrates was determined through the ^{28}Si(d,p) and ^{29}Si(d,p) nuclear reactions. The experimental method is described in detail in the work of Vickridge.[35] The shapes of the cross sections were obtained by registering the proton yield emitted by a 98 nm thick SiO_2/GaAs sample as a function of the deuterium beam energy. A 70 keV wide plateau was found below 1850 keV for the $^{28}Si(d,p_1) + {}^{29}Si(d,p_2)$ reaction cross section, which gave a precision lower than 4% for Si contents below 3.3×10^{18} cm^{-2} (equivalent to 1.5 μm of 2.2 g/cm^3 dense SiO_2). A stoichiometric Si_3N_4 thin film reference grown on GaAs by DECR−PECVD (Distributed Electron Cyclotron Resonance−Plasma-Enhanced CVD) was used as silicon reference target.

Results and Discussion

Hydrogen Incorporation. Figure 1 shows a typical IR spectrum corresponding to a SiO_xH_y film obtained by SiH_4/O_2 CVD, with a thickness of 1.0 μm. This spectrum presents the following absorption bands: three bands at 1072, 810, and 448 cm^{-1}, corresponding to three different vibration modes of the Si−O−Si structures (stretching, bending, and rocking motions, respectively);[36−38] a weak and wide absorption band at 3640 cm^{-1}, associated with the stretching vibration of O−H bonds;[2] a narrow band at 608 cm^{-1}, associated with multiphononic excitations of the Si substrate;[39] a band

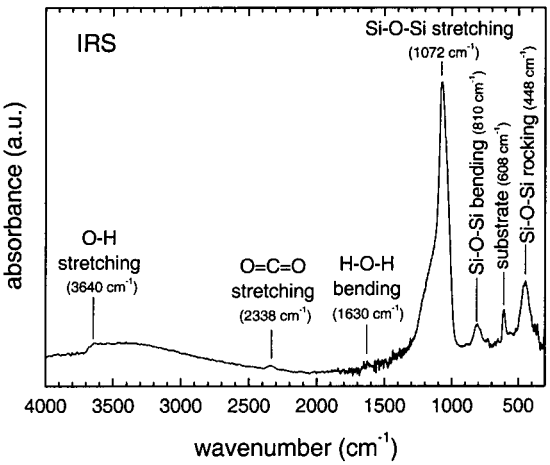

Figure 1. Infrared spectrum of a 1.0 μm thick SiO_xH_y film prepared by SiH_4/O_2 CVD under the following conditions: temperature, 410 °C; total pressure, 1.4 Torr; $[O_2]$:$[SiH_4]$ flow ratio, 15; total gas flow rate, 150 sccm.

at 2338 cm^{-1}, owing to the presence of CO_2 molecules during the IR measurements;[40] and a weak band at 1630 cm^{-1}, corresponding to the bending vibration of H_2O molecules.[41] The asymmetric shape of the main Si−O−Si band (1072 cm^{-1}) is known to proceed from the overlapping of two pairs of longitudinal and transversal optical vibration modes.[3,5,39]

Within a set of IR spectra corresponding to films as thick as 3.2 μm prepared under a wide range of experimental conditions (i.e., temperature = 325−800 °C, $[O_2]$:$[SiH_4]$ flow ratio = 1−25, and total gas flow rate = 100−500 sccm; total pressure = 1.4 Torr in all cases), the stretching Si−H absorption band, typically located at 2270 cm^{-1} in SiO_2,[42] was always absent. To detect this weak Si−H band in the IR spectra, we have prepared a series of very thick samples in the 6−57 μm range, at low (338 °C) and high (450 °C) temperature. The deposition rate was set to the same value (∼ 20 nm/min) for both temperatures by using different total gas flow rates, 250 sccm at 338 °C and 50 sccm at 450 °C, which allows us to analyze individually the effect of the deposition temperature on the hydrogen bonding and concentration with independence on the deposition rate variation that otherwise would be associated with such temperature difference.[24] In both cases, total pressure was maintained at 1.4 Torr and $[O_2]$:$[SiH_4]$ flow ratio at 20.

Figure 2 shows two IR spectra corresponding to the thickest SiO_xH_y films grown at 338 and 450 °C, with thickness of 45.5 μm and 57 μm, respectively. The asymmetric O−H band observed in both spectra at 3640 cm^{-1} corresponds mostly to SiOH groups, although part of the low wavenumber absorption could proceed from H_2O molecules embedded into the oxide matrix (see the discussion below for details). The Si−H bonding, found at 2264 cm^{-1}, is only significant at low temperature.

A measure of the bulk concentration of hydrogenated groups (XH, with X = O or Si) can be obtained from the

(31) Amsel, G.; Nadai, J. P.; d'Artemare, E.; David, D.; Girard, E.; Moulin, *J. Nucl. Instr. Methods* **1971**, *92*, 481.
(32) Chu, W. K.; Mayer, J. W.; Nicolet, M.-A.; Buck, T. M.; Amsel, G. *Thin Solid Films* **1973**, *17*, 1.
(33) Abel, F.; Quillet, V.; Schott, M. *Nucl. Instr. Methods B* **1995**, *105*, 86.
(34) Quillet, V.; Abel, F.; Schott, M. *Nucl. Instr. Methods B* **1993**, *83*, 47.
(35) Vickridge, I. C. *Nucl. Instr. Methods B* **1988**, *34*, 470.
(36) Schumann, L.; Lehmann, A.; Sobotta, H.; Riede, V.; Teschner, U.; Hübner, K. *Phys. Stat. Sol. (b)* **1982**, *110*, K69.
(37) Lucovsky, G.; Yang, J.; Chao, S. S.; Tyler, J. E.; Czubatyj, W. *Phys. Rev. B* **1983**, *28*, 3225.
(38) Pai, P. G.; Chao, S. S.; Takagi, Y.; Lucovsky, G. *J. Vac. Sci. Technol. A* **1986**, *4*, 689.
(39) Lange, P.; Windbracke, W. *Thin Solid Films* **1989**, *174*, 159.
(40) Nakamoto, K.; *Infrared and Raman Spectra of Inorganic and Coordination Compounds*, 4th ed.; John Wiley & Sons: New York, 1986.
(41) Davis, K. M.; Tomozawa, M. *J. Non-Crystalline Solids* **1996**, *201*, 177.
(42) Adams, A. C.; Alexander, F. B.; Capio, C. D.; Smith, T. E. *J. Electrochem. Soc.* **1981**, *128*, 1545.

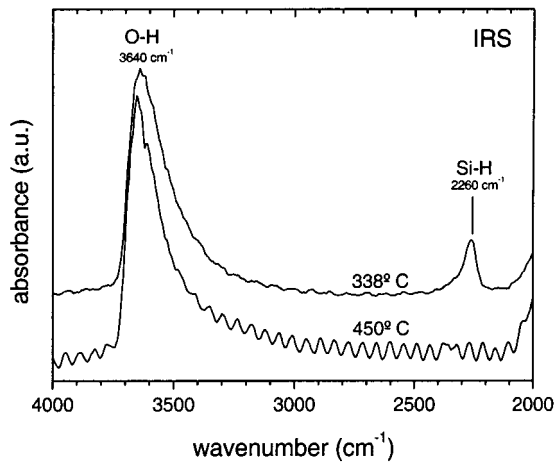

Figure 2. Si−H and O−H IR absorption bands for 45.5 and 57 μm thick SiO_xH_y films prepared at low (338 °C) and high (450 °C) temperature, respectively, under the following conditions: total pressure, 1.4 Torr; $[O_2]$:$[SiH_4]$ flow ratio, 20; total gas flow rate, 250 sccm for 338 °C and 50 sccm for 450 °C. The oscillations observed in both spectra proceed from optical interferences at the oxide film.

ratio between the number of X−H and Si−O−Si bonds per unit area, given by the following approximate equation:[43]

$$\mathrm{XH{:}SiOSi} = \frac{k_{\mathrm{X-H}} \cdot \int_{\mathrm{X-H}} A(\nu)\, \mathrm{d}\nu}{k_{\mathrm{Si-O-Si}} \cdot \int_{\mathrm{Si-O-Si}} A(\nu)\, \mathrm{d}\nu}$$

where $A(\nu)$ is the IR absorbance spectrum, after subtraction of the baseline, as a function of the wavenumber, ν. The integrals of the O−H, Si−H, and Si−O−Si bonds were calculated for the 3640, 2264, and 1072 cm^{-1} bands described above, respectively. k_{O-H} was determined to be 6.2×10^{16} cm^{-1} by comparing ERDA, ^{16}O-$(d,p_1)^{17}O$ NRA, and IRS measurements taken from the thickest high-temperature film (57 μm). According to ref 42, we assumed $k_{Si-H} = 10 \times 10^{16}$ cm^{-1}. Finally, $k_{Si-O-Si}$ was determined from the slope of the curve representing the total content of oxygen atoms, as measured by ^{16}O-$(d,p_1)^{17}O$ NRA, as a function of the integral of the Si−O−Si band at ~1070 cm^{-1}. This calculation involved a set of nine samples prepared under a wide range of experimental conditions and yielded $k_{Si-O-Si} = (1.41 \pm 0.03) \times 10^{16}$ cm^{-1}, which is in good agreement with values reported in other works.[44,45]

The concentrations of OH groups (including both SiOH and H_2O species) found at both temperatures are very similar, with OH:SiOSi bond ratios of 0.168 and 0.146 for the low- and high-temperature films, respectively. The Si−H bonds were only measurable for films thicker than ~10 μm grown at low temperature, for which we obtained a low SiH:SiOSi bond ratio of just 0.016 (i.e., SiH:OH = 0.09). Despite the predominance of the O−H hydrogen bonding, SiH groups may play an important role during the oxide growth. The fact that these groups are eliminated upon increasing the deposition temperature could respond to their rapid conversion into SiOH groups during the film growth.[7] This hypothesis is consistent with molecular orbital calculations on Si−O−H and Si−H bonded clusters,[46] which show that SiOH groups are more stable than SiH ones. In agreement with these results, the insertion of an O atom between a Si−H bond has been reported to be an energetically favorable process in silane clusters and hydrogenated silicon surfaces.[47]

Location and Bonding of the OH Groups. The asymmetric shape of the O−H bands shown in Figure 2 proceeds from two fundamental contributions: (1) the presence of SiOH clusters consisting of two or more interacting (vicinal) SiOH groups with different degrees of bonding strength between them[41,48−50] and (2) the presence of molecular water in different configurations.[41] Isolated and geminal SiOH groups trapped into the oxide matrix (nondistinguishable from each other by IRS)[19] give absorption around 3650 cm^{-1},[7] representing the strongest signal in our spectra. Vicinal SiOH groups with increasing degrees of interaction, either trapped into the oxide matrix or located at surface sites, contribute to the low-frequency asymmetry of our SiO−H band, giving absorption at frequencies ranging from 3650 to 3520 cm^{-1}, depending on their mutual interaction strength.[41,48−50] Free and H-bonded H_2O molecules embedded into the oxide matrix could contribute to the 3425−3225 cm^{-1} range[41] of our O−H band. This band is wider at low temperature, with a fwhm of 176 cm^{-1} against 148 cm^{-1} for the high-temperature sample, which indicates a higher clustering degree of SiOH groups at low temperature and/or a higher incorporation of H_2O molecules. Isolated and geminal SiOH surface groups, normally found around 3750 cm^{-1},[7,48,50] are absent in our spectra.

The short-range chemical environment of the protonated ^{29}Si nuclei in the SiO_xH_y films has been studied in detail by means of CP/MAS NMR. It is worthy to mention that this technique provides an enhanced sensitivity to the protonated ^{29}Si nuclei (i.e., to those forming part either of SiOH or SiH groups) with detriment to the nonprotonated ones (i.e., those at SiOSi groups). Figure 3 shows two NMR spectra corresponding to films prepared under the same conditions exposed above, i.e., at low (338 °C) and high temperature (450 °C). The high-temperature sample exhibits the most resolved spectrum, with two well-defined peaks at −107.2 and −99.9 ppm, corresponding to Q_4 (SiO_4) and Q_3 (isolated SiOH respectively $HOSiO_3$) structures, respectively.[19,51] By contrast, the broader spectrum of the low-temperature film denotes a much higher degree of interaction between the protonated ^{29}Si nuclei (SiOH groups), in agreement with the IRS results. Although less significant, a band around −80 ppm can also be observed in this low-temperature spectrum, which could be attributed to the SiH species detected in the corresponding IR spectrum (Figure 2).[52,53] For both temperatures, a small peak around −93 ppm, which could be

(43) Adams, A. C. *Solid State Technol.* **1983**, April, 135.
(44) Zacharias, M.; Drüsadau, T.; Panckow, A.; Freistedt, H.; Garke, B. *J. Non-Cryst. Solids* **1994**, *169*, 29.
(45) Trchová, M.; Zemek, J.; Jurek, K. *J. Appl. Phys.* **1997**, *82*, 3519.
(46) Kanashima, T.; Okuyama, M.; Hamakawa, Y. *Jpn. J. Appl. Phys.* **1997**, *36*, 1448.
(47) Sun, Q.; Yu, J. Z.; Zhou, L.; Li, Z. Q.; Tang, Z.; Ohno, K.; Kawazoe, Y. *Europhys. Lett.* **1998**, *43*, 47.
(48) Peri, J. B. *J. Phys. Chem.* **1966**, *70*, 2937.
(49) Shelby, J. E. *J. Non-Cryst. Solids* **1994**, *179*, 138.
(50) Sauer, J.; Ugliengo, P.; Garrone, E.; Saunders: V. R. *Chem. Rev.* **1994**, *94*, 2095.
(51) Schilling, F. C.; Steiner, K. G.; Obeng, Y. S. *J. Appl. Phys.* **1995**, *78*, 1303.

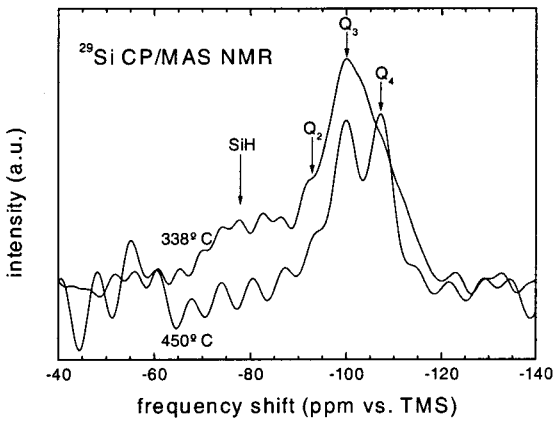

Figure 3. ^{29}Si CP/MAS NMR spectra corresponding to films grown at low and high temperature prepared under the conditions described in the previous figure.

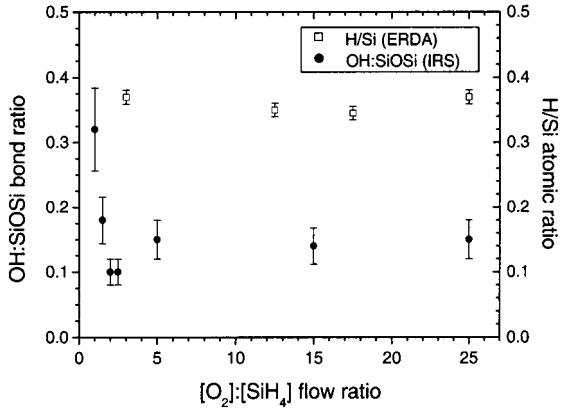

Figure 4. Influence of [O_2]:[SiH_4] flow ratio on the OH concentration, as determined by IRS, and H/Si atomic ratio, as determined by ERDA, in the resulting SiO_xH_y films.

assigned to Q_2 (geminal SiOH respectively $(HO)_2SiO_2$) structures,[19,54] seems to be present. However, this peak becomes too confused with the spectra noise to guarantee the reliability of this assignment. In conclusion, NMR results support that hydrogen atoms are mostly arranged in isolated and interacting SiOH groups, with a negligible or less important contribution of SiH and geminal SiOH groups. Moreover, the proportion of interacting SiOH groups, i.e., the degree of SiOH clustering, is higher at low temperature in comparison with the high-temperature conditions, in accordance with the IRS results.

As it follows from the IR spectra, isolated SiOH groups are trapped into the oxide matrix. However, neither IRS nor NMR results allow us to determine unambiguously whether the interacting SiOH groups are exclusively trapped into the growing film or partially located at surface sites, that is, whether the SiOH clustering occurs exclusively in the film bulk or partially at the surface of a supposed porous structure. This question is directly related to the film compactness, a complex issue not clarified to date and supposedly affected by the incorporation of SiOH and H_2O groups into the oxide matrix.[2−5] In a recent study on SiO_2 thin films grown by SiH_4/O_2 thermal CVD,[55] Dultsev et al. observed by adsorption porometry the formation of open nanopores (2.7−10 nm in radius) occupying up to 15−20% of the film volume, although for a lower deposition temperature (150 °C), higher SiH_4 partial pressures (0.33−0.8 Torr), and a lower [O_2]:[SiH_4] ratio (0.5) than those used by us (338−450 °C, 0.02 Torr, and 20, respectively). They attributed this porous structure to the codeposition of silica nanoparticles previously formed in the gas phase. Under our conditions, we have observed by high-resolution transmission electron microscopy (HRTEM) that SiH_4/O_2 CVD leads to compact amorphous SiO_2 films with a homogeneous microstructure, even at 338 °C, that is, with no evidence for the formation of pores or voids.[56] Refractive index measurements obtained by ellipsometry are in good agreement with these observations.[56] Through a study based on temporal and spatial analysis of atomic force microscopy (AFM) images,[57] we have found that such a compact growth obeys the high surface mobility of the adsorbed film precursor species, which are able to smooth the surface morphology over distances above 60 nm, counteracting the shadowing effects resulting from the random walk of the impinging species around the rough film surface. The lower temperatures used by Dultsev et al. imply a lower surface mobility and the higher SiH_4 partial pressures and lower [O_2]:[SiH_4] ratio a higher formation of silica nanoparticles in the gas phase, both effects being coherent with the porous structure found by these authors. Thus, under our conditions, SiOH clustering is expected to occur predominantly in the film bulk rather than in a supposedly porous surface. This picture is compatible with the IRS results, basically because we have not detected isolated SiOH surface groups.

The decrease of the SiOH clustering degree observed when increasing the deposition temperature can be understood considering that, during the growth of silica, SiOH surface groups are preferential sites for adsorption and reaction in comparison with other surface sites commonly present at silica surfaces under similar conditions,[16] mostly non- or slightly strained siloxane bridges (≡Si−O−Si≡). In this way, at low temperature, those hydrogenated species becoming trapped by the growing film are more likely to appear in interacting configurations forming SiOH clusters. However, at high temperature, the surface mobility of the adsorbed hydrogenated species and the dehydroxylation reactions between adjacent SiOH groups are enhanced, which should retard the formation and further growth of SiOH clusters during the deposition process, as our experiments suggest.

Influence of [O_2]:[SiH_4] Flow Ratio. The OH:SiOSi bond ratio, as deduced from eq 1, and the H/Si atomic ratio (y coefficient in SiO_xH_y as measured by ERDA) were obtained for different [O_2]:[SiH_4] flow ratios during the CVD process, ranging from 1 up to 25. Total pressure was maintained at 1.3 Torr, deposition temperature at 450 °C, and total gas flow rate at 500 sccm. The results are shown in Figure 4, where two regimes

(52) Sindorf, D. W.; Maciel, G. E. *J. Am. Chem. Soc.* **1983**, *105*, 1487.
(53) Brandt, M. S.; Ready, S. E.; Boyce, J. B. *Appl. Phys. Lett.* **1997**, *70*, 188.
(54) Petit, D.; Chazalviel, J.-N.; Ozanam, F.; Devreux, F. *Appl. Phys. Lett.* **1997**, *70*, 191.
(55) Dultsev, F. N.; Nenasheva, L. A.; Vasilyeva, L. L. *J. Electrochem. Soc.* **1998**, *145*, 2569.
(56) To be published.
(57) Ojeda, F.; Cuerno, R.; Salvarezza, R.; Vázquez, L. *Phys. Rev. Lett.* **2000**, *84*, 3125.

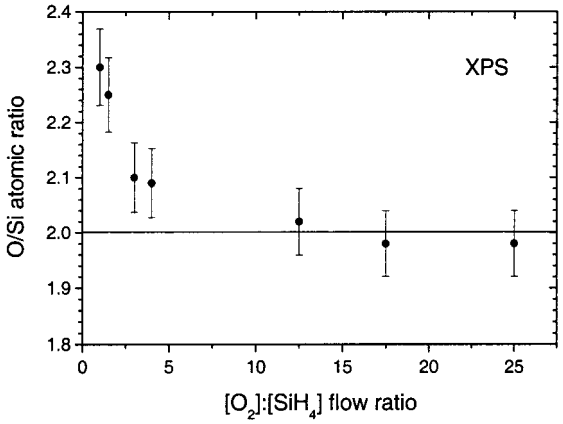

Figure 5. Influence of $[O_2]$:$[SiH_4]$ flow ratio on the O/Si surface atomic ratio, as determined by XPS, in the resulting SiO_xH_y films.

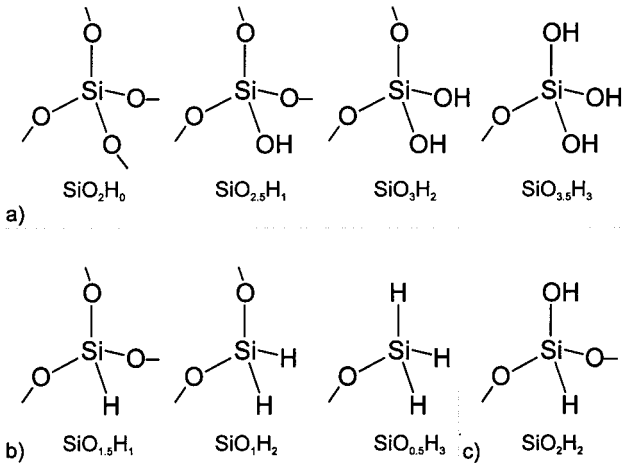

Figure 6. Possible local structures in hydrogenated silicas and their contribution to the oxide stoichiometry.

can be distinguished. For $[O_2]$:$[SiH_4] < 2$, the OH:SiOSi bond ratio decreases rapidly with increasing $[O_2]$:$[SiH_4]$ ratio. The OH:SiOSi bond ratio remains constant for $[O_2]$:$[SiH_4]$ larger than 2, where the H/Si atomic ratio is also nearly constant. Note that in this region the IRS and ERDA data satisfy reasonably the expected relation H/Si = 2OH:SiOSi. Reliable measurements of the H/Si ratio were only possible for $[O_2]$:$[SiH_4] > 2$, owing to the important hydrogen loss (>30%) during the ERDA experiments shown by the oxide films with high OH concentration.

The surface composition of the samples prepared at different $[O_2]$:$[SiH_4]$ flow ratios has been studied using XPS. Figure 5 shows the $[O_2]$:$[SiH_4]$ flow ratio dependence of the O/Si atomic ratio. Initially the O/Si atomic ratio of the deposited film decreases with the $[O_2]$:$[SiH_4]$ flow ratio. However, at $[O_2]$:$[SiH_4]$ flow ratios higher than ~15 the composition SiO_2 is obtained. From a qualitative point of view, this behavior is similar to that shown by the OH:SiOSi bond ratio (see Figure 4), which suggests that the composition of the film is largely determined by the concentration of OH groups embedded into it.

The behavior shown by the O/Si ratio in Figure 5 is contrary to that usually observed in SiO_2 CVD, in particular in plasma CVD[58−60] and SiH_4/N_2O thermal CVD systems,[61] where the O/Si ratio decreases as the oxidant partial pressure decreases. In these systems, due to the effect either of the plasma or of the high temperatures, SiH_4 is decomposed in the absence of the oxidant agent, and the silane fragments (SiH_n with n = 0, 1, 2 or 3), being highly reactive unlike SiH_4, lead to the formation of a substoichiometric oxide (SiO_x with $x < 2$) or simply hydrogenated silicon in the limit where the oxidant partial pressure is null. By contrast, under our low-temperature conditions, SiH_4 molecules are not decomposed in the absence of O_2 (SiH_4 decomposition starts above 500 °C),[62,63] since O_2 is needed to initiate the branching-chain reaction through which the film precursor species are formed. In fact, we have observed that for $[O_2]$:$[SiH_4] = 0$ the deposition rate is negligible (nondetectable). Once deposited, the SiO_mH_n precursor species lead to an overstoichiometric oxide (SiO_x with $x > 2$) due to the predominant incorporation of OH groups into the film (see discussion below). The overstoichiometric character of our films is accentuated as the $[O_2]$:$[SiH_4]$ decreases, because of the increasing concentration of OH groups. In O_2-rich mixtures the dehydrogenation reactions are enhanced,[64] which results in a lower OH concentration and thus in an O/Si ratio closer to 2.

Oxide Stoichiometry. As the XPS/IRS data suggests, the x and y coefficients in the SiO_xH_y formula are not fully independent. For instance, oxides incorporating H atoms exclusively as SiOH groups are formed by $SiO_{4-n}(OH)_n$ structures (n = 0, 1, 2, or 3) (see Figure 6a). All these structures follow a unique chemical formula given by $SiO_{2+0.5y}H_y$, leading to overstoichiometric oxides. In the case of H_2O molecules embedded into the oxide structure, the validity of this formula remains, since the O/H atomic ratio for water is 0.5. Oxides with pure Si−H bonding are formed by $SiO_{4-n}H_n$ structures (n = 0, 1, 2, or 3), which follow the substoichiometric formula $SiO_{2-0.5y}H_y$ (see Figure 6b). In an intermediate situation (e.g., Figure 6c), having both O−H (including SiOH and H_2O species) and Si−H bonds with relative proportions α and β respectively ($\alpha + \beta$ = 1), the oxides are represented by the general formula $SiO_{2+(\alpha-\beta)\times 0.5y}H_y$. Therefore, the O/Si atomic ratio in the oxide film is determined by at least two independent factors, i.e., the total hydrogen concentration (y) and the relative concentration of OH (α) or SiH (β) groups (note that $\alpha - \beta = 2\alpha - 1$). However, in real cases this relationship is more complex due to the presence of other defects. In particular, the presence of −O−O− and −O··· defects in the oxide matrix tends to increase the oxygen-to-silicon ratio in the film, whereas ≡Si−Si≡ and ≡Si··· defects tend to reduce it (the symbol ··· denotes a dangling bond). The different values of the x and y coefficients in the SiO_xH_y formula are represented in Figure 7, which shows two straight lines corresponding

(58) Pan., P.; Nesbit, L. A.; Douse, R. W.; Gleason, R. T. *J. Electrochem. Soc.* **1985**, *132*, 2012.
(59) Han, S. M.; Aydil, E. S. *J. Vac. Sci. Technol. A* **1996**, *14*, 2062.
(60) Sassella, A.; Borghesi, A.; Corni, F.; Monelli, A.; Ottaviani, G.; Tonini, R.; Pivac, B.; Bacchetta, M.; Zanotti, L. *J. Vac. Sci. Technol. A* **1997**, *15*, 377.
(61) Nakamura, M.; Mochizuki, Y.; Usami, K.; Itoh, Y.; Nozaki, T. *J. Electrochem. Soc.* **1985**, *132*, 482.
(62) Bell, T. N.; Perkins, K. A.; Perkins, P. G. *J. Phys. Chem. 1984*, **88**, 116.
(63) Han, J. H.; Rhee, S. W.; Moon, S. H. *J. Electrochem. Soc.* **1996**, *143*, 1996.
(64) Ojeda, F.; Abel, F.; Albella, J. M., to be published.

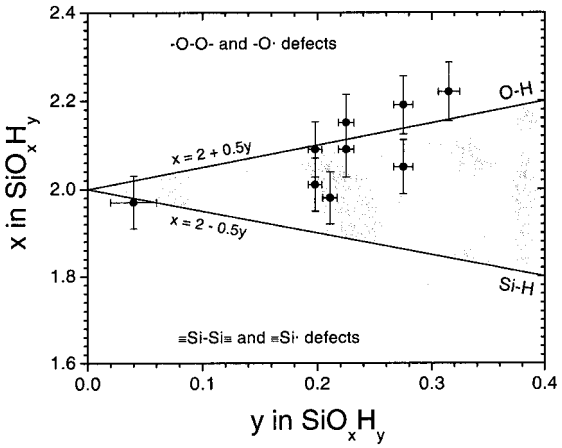

Figure 7. Theoretical relationship between the x and y coefficients in SiO_xH_y films according to the hydrogen bonding and presence of defects in the oxide structure. Solid circles correspond to the experimental x and y coefficients, as determined by NRA and ERDA, respectively, in SiO_xH_y films prepared in a cold-wall reactor.

to oxides containing hydrogen bonded exclusively to oxygen ($x = 2 + 0.5y$) or silicon ($x = 2-0.5y$) atoms. The shadowed area between these two extreme lines limits the zone for oxides with different proportions of O−H, Si−H, oxygen-excess (−O−O− and −O•••) or silicon-excess (≡Si−Si≡ and ≡Si•••) defects, whereas the rest of the area (not shadowed) corresponds to oxides that necessarily have a certain concentration of oxygen- or silicon-excess defects, since these defects provide additional oxygen or silicon atoms over those provided by the OH and SiH groups, respectively.

As a tentative method to determine the chemical formula fitting the composition of the SiO_xH_y films, we plotted the x coefficient (O/Si ratio as measured by XPS) against the y coefficient (H/Si ratio as measured by ERDA). However, this method showed a high dispersion and no evident $x-y$ correlation, which can be explained by the combined use of surface- and bulk-sensitive techniques (XPS and ERDA respectively) and/or to the effect of the lateral inhomogeneities when using different irradiation areas (about 1 cm^2 for XPS against 1 mm^2 for ERDA). To solve these problems, we used RBS (Rutherford backscattering spectroscopy) instead of XPS to measure the O/Si bulk ratio. Although the Si and O levels in the RBS spectra decreased slightly with increasing the hydrogen concentration in the film (due to a decrease of the stopping power), no change was detected in the ratio between the areas behind them, even optimizing the experiment geometry and the signal-to-noise ratio of the spectra. This lack of sensibility of RBS to the O/Si ratio was also observed in simulations performed with the rump code[65] and seems to be a limitation inherent to this technique.

Finally, in an attempt to determine reliably the chemical composition of our films, NRA and ERDA techniques were employed jointly to measure the O/Si (x) and H/Si (y) ratios in a series of samples deposited for this purpose on GaAs wafers in a cold-wall reactor under different conditions (temperatures in the range 370−420 °C and total pressures in the range 3.8−4.5 Torr, maintaining the $[O_2]$:$[SiH_4]$ flow ratio and the total gas flow rates at constant values of 20 and 250 sccm, respectively). We compared these data with those obtained for a SiO_2 film deposited at 450 °C on Ta and further annealed at 700 °C for 4 h in a N_2 atmosphere. This thermal treatment allowed us to obtain a densified SiO_2 sample with a low hydrogen content (H/Si = 0.04 ± 0.02) and a stoichiometric composition (O/Si = 1.97 ± 0.06). NRA and ERDA experiments were performed consecutively in the same chamber, and the deuterium and ^4He ion beams were directed to impinge on the same spot (around 1 mm in diameter) of each sample. In this way we minimize the effect of possible lateral inhomogeneities. The results, which were checked for reproducibility, are presented in Figure 7, showing a fair $x-y$ increasing correlation, with the x and y values falling around the straight line corresponding to a pure O−H hydrogen bonding. Therefore, these results support that the stoichiometry of our films is determined to a large extent by the bulk concentration of OH groups and demonstrate the capability of the NRA/ERDA method to determine precisely the stoichiometry of silica films grown by CVD.

Conclusions

Hydrogen incorporation into SiH_4/O_2 CVD silica films and their stoichiometry have been investigated by IRS, ^{29}Si CP/MAS NMR, XPS, NRA, and ERDA. From NMR/IRS results it follows that SiOH groups are mostly incorporated in isolated and interacting configurations, with a much smaller concentration of geminal SiOH groups. Isolated and interacting (clustered) SiOH groups seem to be trapped into the oxide matrix rather than covering a supposed porous surface. The clustering degree of the SiOH groups decreases with increasing the deposition temperature, which could respond to the increasing rate of the dehydroxylation reactions between the adjacent SiOH groups and to the increasing mobility of the hydrogenated species adsorbed on the growing film surface (plausibly SiO_mH_n species and water molecules). SiH groups, probably due to their high reactivity, are incorporated in a low proportion with respect to the OH groups. In accordance with the predominance of O−H over Si−H bonding, XPS results indicate that the film surface has an overstoichiometric character (i.e., $x > 2$ in SiO_xH_y) which, from a qualitative standpoint, is accentuated as the bulk OH concentration increases. The oxide stoichiometry has been successfully determined by means of a novel method based on NRA/ERDA measurements, which was demonstrated to have a much higher sensibility to the small departures that suffer SiO_2 CVD films from the stoichiometric composition than others methods frequently used in SiO_2 characterization, typically combinations of XPS or RBS and ERDA or IRS. NRA/ERDA results have confirmed that the oxide stoichiometry is determined by the OH concentration in the film.

Acknowledgment. This work was partially supported by the ECSC 7220-ED/082 project and by the 07M/0710/97 project from Comunidad Autónoma de Madrid (CAM). One of us (F.O.) also gratefully acknowledges the grant financed by CAM (683/96, BOCM 22/4/96).

CM011040K

(65) Computer Graphics Service, Cornell University.